JOURNAL OF SOLID STATE CHEMISTRY 104, 368–376 (1993)

Magnetism of (Fe,Co)-Based Alloys with the $La_6Co_{11}Ga_3$-Type

F. WEITZER, A. LEITHE-JASPER, P. ROGL, AND K. HIEBL

Institut für Physikalische Chemie der Universität Wien, Währingerstrasse 42, A-1090, Vienna, Austria

H. NOËL

Laboratoire de Chimie du Solide et Inorganique Moleculaire, Université de Rennes I, U.R.A.-CNRS D0935, Avenue du Général Leclerc, F-35042 Rennes Cedex, France

G. WIESINGER

Institut für Experimentalphysik, Technische Universität Wien, Wiedner Hauptstrasse 8-10, A-1040 Vienna, Austria

AND W. STEINER

Institut für Angewandte und Technische Physik, Technische Universität Wien, Wiedner Hauptstrasse 8-10, A-1040 Vienna, Austria

Received May 26, 1992; in revised form October 29, 1992; accepted November 2, 1992

Alloys with the composition $RE_6(Fe,Co)_{13}X$ (RE = La, Pr, Nd, Sm; X = As, In, Sn, Sb, Tl, Pb, Bi) have been synthesized by the arc melting technique, followed by annealing at 873–1273 K for up to 170 hr in evacuated silica capsules. From room temperature X-ray powder diffraction analysis the alloys were found to crystallize with the ordered $La_6Co_{11}Ga_3$, i.e., the $Nd_6Fe_{13}Si$ type of structure. Precise atom parameters and interatomic distances have been derived from a single crystal X-ray refinement of $Pr_6Fe_{13}Pb$. The $La_6Co_{13}X$ compounds exhibit ferromagnetism with a saturation moment of $\mu_S \sim 1\mu_B$/cobalt atom. From the magnetic behavior of the iron-containing samples antiferromagnetic coupling of at least two magnetic sublattices is concluded to be present because of the strongly reduced magnetization values. While the ^{57}Fe Mössbauer spectra are essentially unaffected by the specific element X, a modified shape of the spectra is observed if the rare earth element is changed. In the case of RE = Nd the spectra indicate an easy c-axis of magnetization in the whole range between room and liquid helium temperature; in the case of RE = Pr a spin reorientation is anticipated.

1. Introduction

In our systematic search for iron-based permanent magnet materials with the early rare earth elements, we have recently reported (*1–3*) on the phase equilibria in the ternary systems Pr–Fe–X, where X was a metal from the third group, Al, Ga, In, and Tl. In all these systems a ternary compound was observed with a peritectic mode of formation at a composition $RE_6Fe_{13-x}X_{1+x}$ with a variable homogeneous range (*1, 2*). These compounds were all found to be isotypic with the structure type of $La_6Co_{11}Ga_3$ (*4*) or $Nd_6Fe_{13}Si$ (*5*) and a general stabilization of this structure type with the early rare earth elements and iron or cobalt by a metametal X = Al, Ga, In, Tl, Ge, Sn, Pb, Sb, and Bi was suspected and confirmed (*1*). In the present paper we report on the range of exis-

0022-4596/93 $5.00

tence, the crystal chemistry, and the magnetic properties of these new compounds as investigated by X-ray analysis and by magnetic susceptibility and magnetization measurements in the temperature range from 5 to 800 K. Finally the ^{57}Fe Mössbauer spectra were recorded between ambient temperature and 4.2 K. The properties of the Al,Ge-containing phases are the subject of a paper published recently (*6*).

2. Experimental Details

The samples, each with a total weight of ca. 1 g, were prepared by arc melting from ingots and compacted powders of the constituting elements starting from a nominal composition of at.% *RE*(30.5)(Fe,Co)(64.5) *X*(5) or *RE*(30)Fe(55)Ga(15). Materials used were commercially available as high purity elements: rare earths were in the form of ingots (99% pure, Auer–Remy GmbH., FRG); lumps of iron (99.9% pure) and specpure Co in the form of rods were supplied by Johnson Matthey & Co., U.K.; Ga (99.9%) was obtained as an ingot from Alcan Electronics, Switzerland. In, Tl, Sn, Pb, As, Sb, and Bi were all used as 99.9% pure ingots from Johnson Matthey & Co., U.K. To ensure homogeneity the samples were remelted several times using electric currents as low as possible to minimize weight losses by evaporation. Weight losses were compensated for beforehand by extra amounts of Sm or the metametal *X*, respectively. The reguli were then wrapped in Mo-foil, sealed in evacuated quartz tubes, and annealed for 75 to 170 hr at various temperatures in the range from 873 to 1273 K (for details see Table I). After heat treatment the alloys were quenched by submerging the silica tubes in water.

Lattice parameters and standard deviations were obtained by a least-squares refinement of room temperature 114.59 mm Debye–Scherrer or Guinier–Huber X-ray powder data, using Cr$K\alpha$ or monochromatized Cu$K\alpha_1$-radiation with an internal standard of 99.9999% pure Ge (a_{Ge} = 0.5657906 nm).

Due to a general instability of the alloys and in particular of the iron-containing La-base compounds with respect to rapid hydrolysis in moist environments, handling of the specimens in most cases was performed in an argon-filled glovebox system ensuring levels of less than 2 ppm O_2 and less than 4 ppm H_2O.

Magnetization curves at various temperatures were recorded by a Faraday balance down to liquid nitrogen temperatures and with a SQUID magnetometer down to 5 K and fields up to 3 T. Curie temperatures were determined in low external fields.

The Mössbauer spectra were recorded between 295 and 4.2 K using a conventional constant acceleration type spectrometer with a ^{57}Co source in a rhodium matrix. The data were analyzed by applying a least-squares fit procedure under the assumption of a discrete superposition of Lorentzian lines. The number of the subspectra was constrained to the different Fe-lattice sites. The line width was kept equal for all lines occurring in a pattern. The isomer shift data are given relative to α-Fe at room temperature.

3. Results and Discussion

3.1. Compound Formation and Structural Chemistry

X-ray powder analysis of the annealed alloys revealed the existence of a new ternary phase whose X-ray powder intensity patterns closely resembled the one observed for $Pr_6Fe_{11}Ga_3$ earlier obtained in a reinvestigation of the phase equilibria in the Fe-rich region of the Pr–Fe–Ga ternary system (*2*). From the investigated ternary combinations (La, Ce, Pr, Nd, Sm, Gd, and MM)$_6$ Fe$_{13-x}$ (Ga, As, In, Sn, Sb, Tl, Pb, Bi)$_{1+x}$ compound formation in the investigated temperature range 600 to 800°C was never encountered with Ce, mischmetal (MM), and the rare earth elements equal or smaller in size than Gd.

TABLE I

CRYSTALLOGRAPHIC AND MAGNETIC DATA FOR TERNARY ALLOYS RE – Fe/Co – X (RE = La, Ce, Pr, Nd, AND Sm; X = Ga, As, In, Sn, Sb, Tl, Pb, AND Bi) SPACE GROUP $I4/mcm$, $Nd_6Fe_{13}Si$ – TYPE OR $La_6Co_{11}Ga_3$ – TYPE RESPECTIVELY

Phase	Preparation technique	Unit cell dimensions in nm					T_c (K)	σ_s Am²/kg	M_s μ_B/f.u.	μ_s μ_B/Co	θ_p (K)	μ_{eff} μ_B/f.u.
		a	b	c	c/a	V						
$La_6Fe_{13}Sn$	873 K, 5 days	0.8148(1)	—	2.4047(8)	2.951	1.5966(7)						
$La_6Fe_{13}Pb$	873 K, 5 days	0.8155(2)	—	2.4123(7)	2.958	1.6043(5)						
$La_6Co_{13}In$	1053 K, 5 days	0.8102(2)	—	2.3576(8)	2.910	1.5474(5)	490	37.5	11.5	0.9		
$La_6Co_{13}Tl$	873 K, 5 days	0.8087(1)	—	2.3548(8)	2.912	1.5399(6)	340	41.3	13.3	1.0		
$La_6Co_{13}Sn$	973 K, 5 days	0.8096(1)	—	2.3461(7)	2.898	1.5379(6)	190	46.4	14.3	1.1		
$La_6Co_{13}Pb$	973 K, 5 days	0.8101(1)	—	2.3533(8)	2.905	1.5446(7)	140	38.0	12.3	0.9		
$La_6Co_{13}Sb$	1073 K, 5 days	0.8097(1)	—	2.3289(8)	2.876	1.5268(7)	490	44.5	13.7	1.1		
$La_6Co_{13}Bi$	1073 K, 7 days	0.8114(2)	—	2.3477(9)	2.894	1.5456(9)						
$Pr_6Fe_{11}Ga_3$	1053 K, 5 days	0.8099(1)	—	2.3084(11)	2.850	1.5140(9)	320	32.0	9.6		312	14.6
$Pr_6Fe_{13}In$	1053 K, 5 days	0.8103(1)	—	2.3527(9)	2.893	1.5449(8)	290	26.2	8.0		355	19.5
$Pr_6Fe_{13}Tl$	1053 K, 5 days	0.8097(1)	—	2.3509(10)	2.903	1.5413(8)	280	21.8	6.9		371	17.8
$Pr_6Fe_{13}Sn$	1053 K, 5 days	0.8098(1)	—	2.3471(9)	2.898	1.5393(8)	250	7.9	2.4			
$Pr_6Fe_{13}Pb$	1053 K, 5 days	0.8106(1)	—	2.3565(9)	2.907	1.5483(8)	420	7.1	2.3			
$Pr_6Fe_{13}As$	1073 K, 5 days	0.8059(2)	—	2.2767(6)	2.825	1.4785(8)						
$Pr_6Fe_{13}Sb$	1273 K, 2 days	0.8108(1)	—	2.3303(7)	2.874	1.5317(6)	450	6.8	2.1			
$Pr_6Fe_{13}Bi$	1073 K, 5 days	0.8116(1)	—	2.3516(7)	2.898	1.5489(7)						
$Nd_6Fe_{13}In$	1053 K, 5 days	0.8088(1)	—	2.3431(9)	2.897	1.5327(7)	330	39.9	12.2		403	19.0
$Nd_6Fe_{13}Tl$	1053 K, 5 days	0.8089(1)	—	2.3381(9)	2.891	1.5298(8)	330	36.7	11.8		402	18.7
$Nd_6Fe_{13}Sn$	1053 K, 5 days	0.8089(1)	—	2.3354(9)	2.887	1.5282(7)	510	22.8	7.0			
$Nd_6Fe_{13}Pb$	1053 K, 5 days	0.8092(1)	—	2.3452(8)	2.898	1.5358(7)	330	29.4	9.5			
$Nd_6Fe_{13}As$	1053 K, 5 days	0.8049(2)	—	2.2665(4)	2.816	1.4683(8)						
$Nd_6Fe_{13}Sb$	1073 K, 7 days	0.8098(1)	—	2.3232(7)	2.868	1.5233(7)	550	7.8	2.4			
$Nd_6Fe_{13}Bi$	1073 K, 7 days	0.8103(1)	—	2.3417(6)	2.889	1.5375(6)	510	8.1	2.6			
$Sm_6Fe_{13}In$	1053 K, 5 days	0.8065(1)	—	2.3202(6)	2.877	1.5090(7)						
$Sm_6Fe_{13}Tl$	1053 K, 5 days	0.8055(1)	—	2.3162(8)	2.875	1.5029(7)	380	25.2	8.3			
$Sm_6Fe_{13}Sn$	1053 K, 5 days	0.8055(1)	—	2.3170(9)	2.877	1.5032(6)						
$Sm_6Fe_{13}Pb$	1053 K, 5 days	0.8056(1)	—	2.3265(9)	2.888	1.5099(7)						
$Sm_6Fe_{13}Sb$	1073 K, 3 days	0.8041(1)	—	2.3048(6)	2.866	1.4902(5)						
$Sm_6Fe_{13}Bi$	1073 K, 4 days	0.8057(1)	—	2.3316(8)	2.899	1.5195(9)						

Indexing of the X-ray powder patterns was possible on the basis of a tetragonal unit cell (see Table I). Systematic extinctions observed were based on a body centered Bravais lattice type and on the reflections ($0kl$) with $k, l \neq 2n$ compatible with the $La_6Co_{11}Ga_3$-type (*4*) or with the ordered version, i.e., the $Nd_6Fe_{13}Si$-type (*5*). Employing the atom parameter set obtained from the single crystal refinement of $Pr_6Fe_{13}Pb$ (see Section 3.2), in the calculation of the X-ray powder intensities, good agreement with the experimentally observed intensities is obtained in all cases, thereby confirming the isotypy.

As observed from multiphase Nd–Fe–Sb alloys, there was considerable variation of the c-parameters of the $Nd_6Fe_{13}Sb$ phase. Homogeneity ranges therefore are nonnegligible at the temperatures investigated. Except for $Pr_6Fe_{11}Ga_3$ in all other cases studied the stoichiometry was $RE_6(Fe,Co)_{13}X$. Sample preparation of the Sm-containing alloys proved to be difficult, due to severe Sm-losses in the arc melting process as well as during homogenization treatment. We thus failed to achieve homogeneous samples free of secondary impurity phases such as Sm_2Fe_{17} and/or $SmFe_3$.

The variation of the unit cell parameters as a function of the atomic number of the lanthanoid element typically revealed the lanthanoid contraction as well, as it reflects the atomic size relation among the metametals. Due to the variations in the thermodynamic stability of the neighboring equilibrium phases, stabilities of the $RE_6(Fe,Co)_{13}X$ phases decrease along the se-

quence Fe → Co → Ni; i.e., cobalt containing compounds are only observed for lanthanum, whereas no isotypic compounds were observed with Ni.

As far as the thermal stability of the novel phases is concerned, most compounds were found to be stable at $T < 1053$ K and to form in a ternary peritectic (Class III) type of reaction. It should be mentioned, however, that the La-containing phases generally revealed a decomposition temperature lower than 1023 K. $Nd_6Fe_{13}Sb$ obtained at 1073 K was observed to decompose after 14 days at 773 K into Nd_2Fe_{17} and Nd_5Sb_3.

3.2. Single Crystal X-Ray Refinement of the Crystal Structure of $Pr_6Fe_{13}Pb$

A small single-crystal specimen (size 40 × 80 × 160 μm) was obtained by mechanical fragmentation of an arc melted alloy which had been annealed for 80 hr at 1053 K close to its (peritectic) melting point. Examination of Cu$K\alpha$-Weissenberg photographs (axes [100] and [110]) revealed slightly broadened reflections which were consistent with a body centered tetragonal high Laue symmetry. From statistical tests a center of symmetry was obvious, which together with the only observed extinctions ($0kl$) for $k, l \neq 2n$ resulted in $I4/mcm$ as the most probable space group type. No deviations from these extinctions were encountered; however, deviations may have been too weak to be observed owing to the generally broadened nature of the reflections. Integrated intensities were measured with graphite monochromated Mo$K\alpha$ radiation on a STOE automatic four circle diffractometer out to a limit of $\sin\theta/\lambda = 4.8$ nm^{-1}. From the total of 445 recorded intensities, a set of 216 symmetry independent reflections was obtained by averaging centered reflections only (182 for $|F_0| > 3\sigma$). A geometrical absorption correction μ(Mo$K\alpha$) = 39.4 mm^{-1} was applied, describing the crystal surface by three faces (100), (110) and (001). The crystallographic data are listed in Table II. The chemical formula, the unit cell dimensions, space group symmetry, and the close resemblance of the X-ray powder intensities with the structure type of $La_6Co_{11}Ga_3$ suggested refinement using the atom parameters of $La_6Co_{11}Ga_3$ as starting values in the STRUCSY full matrix least squares program system (STOE & Cie, Darmstadt, FRG). Weights used were based upon counting statistics $\omega_i = 1/[(\sigma(F_i)]^2$. Refinement of the atom order and occupancies undoubtedly revealed a fully ordered structure with the Pb-atoms occupying the centers of bicapped Archimedian antiprisms $Pr_{8+2}Pb$ in the same way as Si-atoms were found to occupy the Archimedian antiprisms in $Nd_6Fe_{13}Si$ (5). There was no deviation from full occupancies, and different weighting schemes were of no significant influence on the residual value. The final R-value, calculated with anisotropic thermal parameters (see Table II), was $R = 0.045$ ($R_\omega = 0.041$). At this point a difference map $F_0 - F_c$ was featureless, confirming the isotypy with the crystal structure of $Nd_6Fe_{13}Si$ (*5*) as the fully ordered version of the $La_6Co_{11}Ga_3$-type (*4*). For interatomic distances see Table III. A listing of F_0 and F_c values may be obtained on request.

3.3. Magnetism

Magnetic properties were measured on crushed particles of polycrystalline specimens. The observed magnetic data (ordering temperatures, magnetization and saturation moments, etc.) are summarized in Table I.

The $La_6Co_{13}X$ compounds are ferromagnets and their Curie temperatures strongly depend on the constituting element X. The curves for magnetization at a field of 0.1 T versus temperature are presented in Fig. 1. The observed maxima are obviously due to a spin reorientation according to a canted alignment of the cobalt moments in the four different Co-positions of this structure type. From magnetic isotherms versus field (see inset Fig. 1) we derived the saturation moments per Co atom; the constant value for all samples of $\mu_S \sim 1\mu_B$ is about 40% smaller

TABLE II

CRYSTAL DATA FOR $Pr_6Fe_{13}Pb$ ($Nd_6Fe_{13}Si$-TYPE OR ORDERED $La_6Co_{11}Ga_3$-TYPE)

Atom	Site	x	y	z	U_{11}	U_{22}	U_{33}	U_{12}	U_{13}	U_{23}
Pr1	16l	0.1627(3)	0.6627(3)	0.1857(1)	1.1(1)	1.1(1)	2.6(1)	0.25(13)	0.07(9)	0.07(9)
Pr2	8f	0	0	0.8944(1)	0.45(15)	0.45(15)	2.7(2)	0	0	0
Fe1	16l	0.1795(6)	0.6795(6)	0.0585(2)	0.48(30)	0.48(30)	2.4(3)	0	0.57(21)	0.57(21)
Fe2	16k	0.0659(8)	0.2103(9)	0	0.78(53)	1.0(5)	2.3(3)	0	0	0
Fe3	16l	0.3856(6)	0.8856(6)	0.0936(2)	0.73(30)	0.73(30)	2.4(3)	0.25(30)	0.93(30)	0.93(30)
Fe4	4d	0	½	0	0.17(5)	0.17(5)	2.7(6)	1.2(7)	0	0
Pb	4a	0	0	¼	0.73(16)	0.73(16)	2.6(2)	0	0	0

Note. Space group, $I4/mcm$-D_{4h}^{18}, No. 140, $Z = 4$; origin at center. $a = 0.81059(15)$nm, $c = 2.35648(94)$nm, $c/a = 2.907$, $V = 1.5483(8)$nm^3, $\rho_x = 7.63$ Mg m^{-3}. Anisotropic thermal factors are expressed as $T = \exp[-2\pi^2(U_{11}h^2a^{*2} + U_{22}k^2b^{*2} + U_{33}l^2c^{*2} + 2U_{12}hka^*b^* + 2U_{13}hla^*c^* + 2U_{23}klb^*c^*) \times 10^{-2}]$. The standard deviations are given in parentheses.
Correction for isotropic secondary extinction (Zachariasen) was $g = 2.2(6) \times 10^{-7}$
Residual values: $R_F = 0.049$, $R_w = 0.041$; GOF = 1.76.

than the ones found in, e.g., the 2 : 17 phases (*7*), as well as in the 1 : 13 phases (*8*), and supports the above assumption of a noncollinear spin arrangement ("overt" canting with a net total magnetic moment).

The $(Pr,Nd,Sm)_6Fe_{13}X$ compounds show magnetic behavior affected by the element X (see Fig. 2 and Table I). Since the low temperature magnetization does not exhibit field cooling effects (spin glass behavior), the low overall magnetization is suggested to originate from a ferrimagnetic ordering due to an antiparallel alignment of at least two sublattices (*RE* and/or Fe). Unfortunately it was not possible to obtain reliable measurements from the $La_6Fe_{13}X$ homologues as they were magnetically affected by small amounts of secondary phases, predominantly iron. We thus were not able to estimate the contribution of the iron sublattice to the magnetic moment per unit cell according to the general formula $M_S = |6\mu_{RE} - 13\mu_{Fe}|$.

However, if we use a typical iron moment of $1.5\mu_B < \mu_{Fe} < 2\mu_B$ as usually observed in *RE*–iron-based magnets (*9*) as well as $M_{RE} \sim 3\mu_B$, the low magnetization found in our experiments seems to be plausible. Since the samples start to segregate at temperatures above 500 K, evaluation of the paramagnetic parameters is less reliable (Table I) and does not allow a conclusive determination of the iron magnetic ground state.

Finally the isostructural compound $Pr_6Fe_{11}Ga_3$ was investigated and the results which were found, in good agreement with Li *et al.* (*10*), are added in Table I and show close resemblance to the $RE_6T_{13}X$ alloys, i.e., ferrimagnetism caused by an antiferromagnetic coupling of the rare-earth and iron sublattices, respectively.

TABLE III

INTERATOMIC DISTANCES (<0.400 nm) IN $Pr_6Fe_{13}Pb$, 296 K

Pr1–	1	Fe1	0.3003(5)	Fe2–	1 Fe4 0.2408(7)
	1	Fe3	0.3148(5)		2 Fe1 0.2494(7)
	2	Fe3	0.3352(5)		2 Fe2 0.2527(13)
	2	Pb	0.3393(2)		1 Fe2 0.2565(13)
	2	Pr2	0.3575(2)		2 Fe1 0.2579(7)
	1	Pr1	0.3632(4)		2 Fe3 0.2653(6)
	1	Pr1	0.3730(4)		2 Pr2 0.3063(5)
Pr2–	4	Fe2	0.3063(5)	Fe3–	1 Fe1 0.2503(6)
	4	Fe1	0.3178(4)		1 Fe4 0.2566(5)
	4	Fe3	0.3273(4)		2 Fe1 0.2576(6)
	1	Pb	0.3403(3)		1 Fe3 0.2623(9)
	4	Pr1	0.3575(2)		2 Fe2 0.2653(6)
Fe1–	1	Fe4	0.2477(4)		2 Pr1 0.3148(5)
	2	Fe2	0.2494(7)		2 Pr2 0.3273(4)
	1	Fe3	0.2503(6)		1 Pr1 0.3352(5)
	2	Fe3	0.2576(2)	Fe4–	4 Fe2 0.2408(7)
	2	Fe2	0.2579(7)		4 Fe1 0.2477(4)
	1	Fe1	0.2757(9)		4 Fe3 0.2566(5)
	1	Pr1	0.3003(5)		
	2	Pr2	0.3178(4)	Pb–	8 Pr1 0.3393(2)
					2 Pr2 0.3403(2)

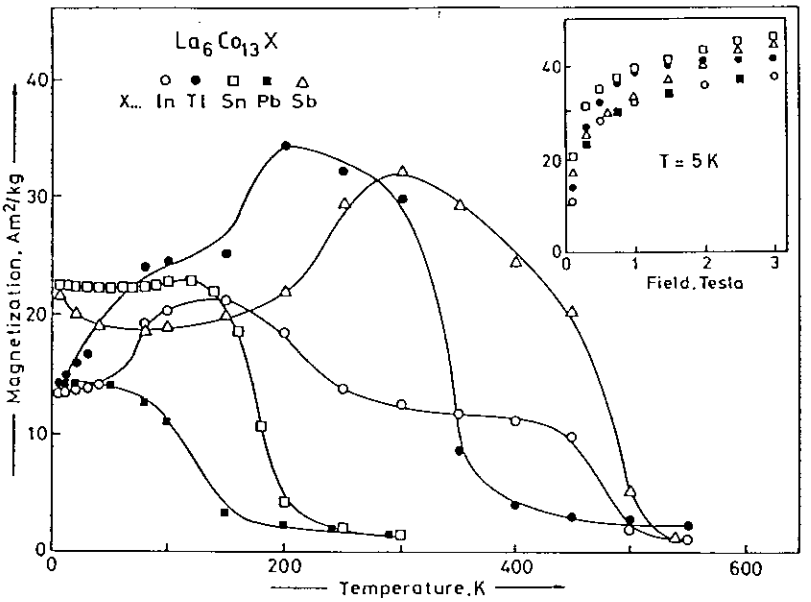

FIG. 1. Magnetization versus temperature for $La_6Co_{13}X$ at a field of 0.1 T. Inset: Field dependent magnetization at $T = 5$ K.

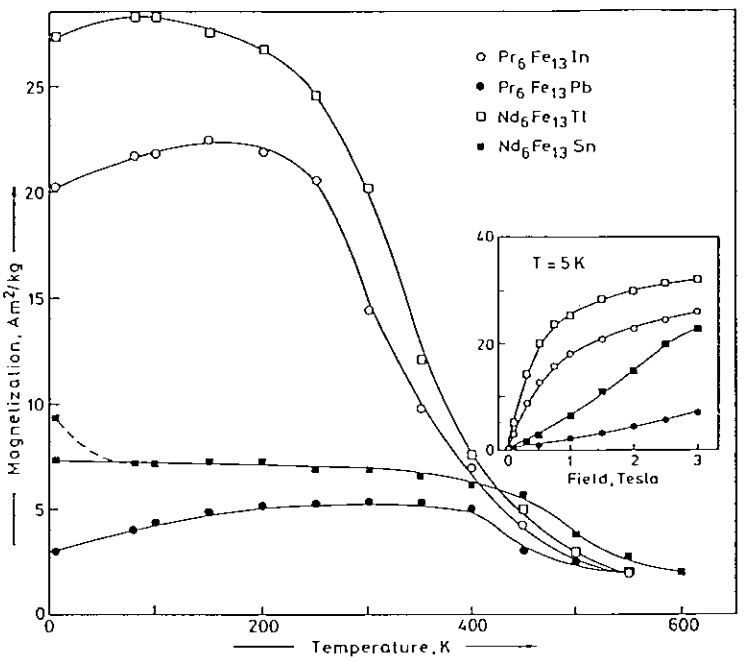

FIG. 2. Magnetization versus temperature for $RE_6Fe_{13}X$ at a field of 1.28 T. Inset: Magnetic isotherms versus field at $T = 5$ K.

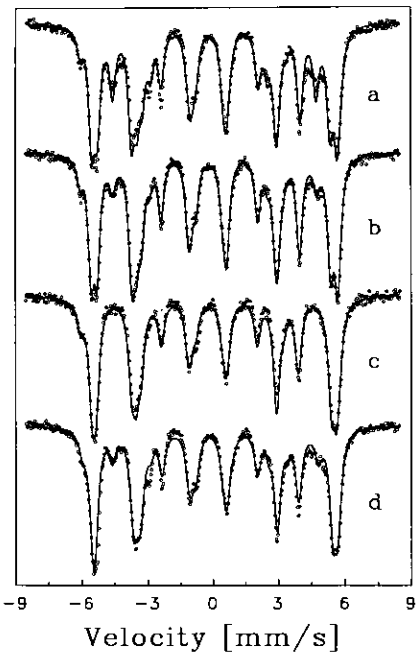

FIG. 3. Mössbauer spectra for $Nd_6Fe_{13}X$ recorded at T = 5 K: (a) X = In; (b) X = Tl; (c) X = Sn; (d) X = Pb; (· · ·) Data points; (———) computer fit as described in the text.

3.4. *Mössbauer Spectroscopy*

Since the unit cell of $RE_6Fe_{13}X$ contains four nonequivalent Fe-lattice sites with the occupation ratio $16(l_1) : 16(l_2) : 16(k) : 4(d)$ (at least when the anisotropic dipole field contributions are ignored), a Mössbauer pattern is expected to consist of four subspectra with identical relative intensities. In the case of an easy c-axis of magnetization the contribution of the dipole fields only changes the absolute values of the hyperfine fields, however leaving the intensity of the subspectra resulting from equivalent lattice sites unchanged. In the case of a deviation of the easy axis from the c-direction, the various dipole field contributions lift the degeneracy of the magnetically equivalent lattice sites, and thus give rise to a splitting of the pattern reflecting a given lattice site into two or three subspectra (*11*).

All the Mössbauer spectra of the Nd-compounds show almost identical features (Fig. 3). In Table IV the hyperfine parameters obtained from the computer fit are listed for the data measured at 4.2 K and at ambient temperature. In some cases traces of Nd_2Fe_{17} could be detected. Generally the spectra were analyzed by choosing the Fe lattice site occupation number as a measure of the intensity ratio. In the case of $Nd_6Fe_{13}Sn$, however, the intensity ratio showed slight deviations from the ideal value, even at 4.2 K, indicating either an incomplete filling of the lattice sites or a slight degree of atomic disorder. For all Nd compounds under investigation the weak spectrum due to the 4d sites is well resolved at the low energy shoulder of line one, and thus can easily be identified. The remaining three Fe lattice sites show identical occupation numbers (l_1, l_2, k). Based on the usual dependency of the hyperfine field at a given lattice site on the number of nearest Fe neighbors (Table III) the following sequence is obtained: $B_{eff}(4d(Fe4)) > B_{eff}$ (16k(Fe2)) $> B_{eff}(16l_1(Fe1)) > B_{eff}(16l_2(Fe3))$. The average interatomic Fe–Fe distances are similar for the different Fe sites; their number, however, varies considerably (12, 10, 9, 7 for Fe4, Fe2, Fe1, Fe3, respectively). Thus, the difference observed for the isomer shift in the case of the two l sites additionally reflects the variation in the number of next nearest Pr atoms (3 and 5 for Fe1 and Fe3, respectively). The large spread of the individual hyperfine field values (35%) is attributed to the great variation of the number of near Fe neighbors. Nevertheless, it would be worthwhile to study the apparent wide distribution of atomic moments by means of neutron scattering experiments. Generally, however, hyperfine field and isomer shift data obtained for the subspectra are strictly correlated: an increase in the hyperfine field is always accompanied by a more negative isomer shift, reflecting a larger s-like electron density at Fe nuclei on sites with a larger hyperfine field.

In order to study the temperature dependence of the hyperfine field more carefully, four $Nd_6Fe_{13}Sn$ spectra were measured in 50 K temperature intervals down to 5 K, yielding a homogeneous and smooth behav-

TABLE IV

HYPERFINE FIELD (B_{eff}), QUADRUPOLE SPLITTING (ΔE_Q) AND CENTER SHIFT (IS) IN $Nd_6Fe_{13}X$

		T = 4.2 K			T = 295 K		
X	Iron Site	B_{eff} [T] ± 0.05	ΔE_Q [mm/s] ± 0.02	IS [mm/s] ± 0.02	B_{eff} [T] ± 0.05	ΔE_Q [mm/s] ± 0.02	IS [mm/s] ± 0.02
In	4 d	36.76	−0.03	0	30.06	0.10	−0.18
	16 k	34.55	0.31	0.03	28.73	0.37	−0.10
	16 l_1	32.87	0.20	0.05	26.71	0.26	−0.09
	16 l_2	23.97	0.27	0.11	19.44	0.32	−0.04
Tl	4 d	36.24	−0.43	0.18	28.76	0.06	−0.27
	16 k	34.41	0.35	0.02	28.45	0.36	−0.09
	16 l_1	32.61	0.19	0.04	26.13	0.29	−0.12
	16 l_2	24.00	0.27	0.12	19.39	0.27	−0.02
Sn	4 d	36.53	0.02	−0.02	29.35	0.05	−0.19
	16 k	34.52	0.34	0	28.43	0.38	−0.10
	16 l_1	33.22	0.21	+0.04	26.48	0.28	−0.10
	16 l_2	23.66	0.26	+0.08	19.28	0.27	−0.04
Pb	4 d	36.31	−0.14	0.10	29.36	0.07	−0.22
	16 k	34.50	0.35	0.01	28.43	0.37	−0.11
	16 l_1	33.18	0.20	0.04	26.51	0.26	−0.09
	16 l_2	23.53	0.27	0.10	19.00	0.25	−0.03

Note. The center shift IS is given relative to α-Fe at room temperature.

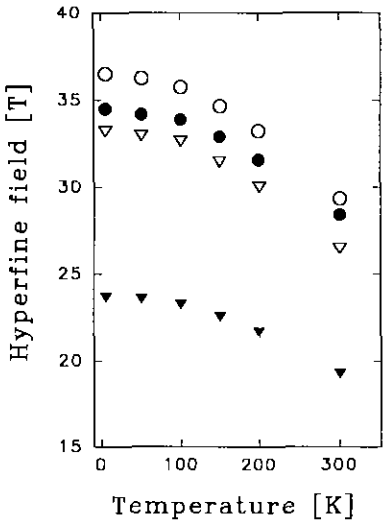

FIG. 4. Hyperfine fields at individual Fe lattice sites versus temperature obtained for $Nd_6Fe_{13}Sn$: (○) 4d; (●) 16 k; (▽) 16 l_1; (▼) 16 l_2.

ior of the four individual hyperfine fields (Fig. 4).

The spectra recorded from the two Pr samples (X = Pb,Sn) were of a rather different shape; the line width has increased, compared to the Nd case. The large spread of the hyperfine data, as observed in the spectra of the Nd compounds, is no longer present, which may be due to the smaller influence of the *RE* amount in the Pr case. Since the samples are crystallographically equivalent, a spin reorientation from the c axis may occur below room temperature, a fact which may also be responsible for the shallow maximum in the magnetization vs. temperature curves. In order to confirm this assumption, Mössbauer measurements at variable temperature are in progress.

Acknowledgments

This research was supported by the Austrian Science Foundation (Fonds zur Förderung der wissenschaftlichen Forschung in Österreich) under Contracts S5604 and S5605. Thanks are furthermore due to the Hochschuljubiläumsstiftung der Stadt Wien. K. Hiebl

and H. Noël are grateful to the CNRS and the Austrian Academy of Sciences for fellowships in Rennes and Wien, respectively.

References

1. F. Weitzer, H. Klesnar, and P. Rogl, "Phase Equilibria and Structural Chemistry Related to (Al,Ga,In,Tl)-Substituted Rare Earth Iron-Base Permanent Magnet Materials," paper presented at the Intl. Conf. Advanced Aluminium and Magnesium Alloys, Amsterdam, The Netherlands (June 20–26, 1990).
2. F. Weitzer and P. Rogl, *J. Less-Common Met.* **167,** 135 (1990).
3. H. Klesnar and P. Rogl, *J. Mater. Res.* **6,** 53 (1991).
4. O. M. Sichevich, R. V. Lapunova, A. N. Sobolev, Yu. N. Grin, and Ya. P. Yarmolyuk, *Sov. Phys. Crystallogr.* **30,** 627 (1985).
5. J. Allemand, A. Letant, J. M. Moreau, J. P. Nozieres, and R. Perrier de la Bathie, *J. Less-Common Met.* **166,** 73 (1990).
6. B. Hu, J. M. D. Coey, H. Klesnar, and P. Rogl, *J. Magn. Magn. Mater.* **117,** 225 (1992).
7. H. Klesnar, K. Hiebl, P. Rogl, and H. Noël, *J. Less-Common Met.* **154,** 217 (1989).
8. F. Weitzer, K. Hiebl, Yu. Grin, P. Rogl, and H. Noël, *J. Appl. Phys.* **68,** 3504 (1990).
9. F. Weitzer, P. Rogl, K. Hiebl, and J. Grin, *J. Appl. Phys.* **68,** 3612 (1990).
10. Hong-Shuo Li, Bo-Ping Hu, J. M. Cadogan, J. M. D. Coey, and J. P. Gavigan, *J. Appl. Phys.* **67,** 4841 (1990).
11. W. Steiner and R. Haferl, *Phys. Status Solidi A* **42,** 739 (1977).